

# Analysis of AC-DC Converter Circuit Performance with Difference Piezoelectric Transducer Array Connection

Nik Ahmad Kamil Zainal Abidin<sup>1\*</sup>, Norkharziana Mohd Nayan<sup>1</sup>, Azuwa Ali<sup>1</sup>, N. A. Azli<sup>2</sup>, N. M. Nordin<sup>2</sup>

<sup>1</sup>Centre of Excellence for Renewable Energy (CERE), School of Electrical Systems Engineering, Universiti Malaysia Perlis, Pauh Putra Campus, 02600 Arau, Perlis, MALAYSIA

<sup>2</sup>Power Electronics and Drive Research Group, School of Electrical Engineering, Universiti Teknologi Malaysia, 81310 Skudai, Johor, MALAYSIA

\*Corresponding Author

DOI: <https://doi.org/10.30880/ijie.2020.12.07.003>

Received 30 March 2020; Accepted 3 August 2020; Available online 30 August 2020

**Abstract:** This research presents a simulation analysis for the AC-DC converter circuit with a different configurations of the array connection of the piezoelectric sensor. The selection of AC-DC converter circuits is full wave bridge rectifier (FWBR), parallel SSHI (P-SSHI) and parallel voltage multiplier (PVM) with array configuration variation in series (S), parallel (P), series-parallel (SP) and parallel-series (PS). The system optimizes with different load configurations ranging from 10 k $\Omega$  to 1 M $\Omega$ . The best configuration of AC-DC converter with an appropriate array piezoelectric connection producing the optimum output of harvested power is presented. According to the simulation results, the harvested power produced by using P-SSHI converter connected with 3 parallel piezoelectric transducer array was 85.9% higher than for PVM and 15.88% higher than FWBR.

**Keywords:** Energy harvesting; vibration; piezoelectric; AC-DC converter circuit

## 1. Introduction

Energy harvesting is a process where energy is captured from the ambient environment converted into electrical sources. In recent years, alternative energy sources are being widely studied due to resource depletion and pollution problem. In order to overcome resource depletion and pollution problems, researchers investigate an alternative way to harness energy from energy harvesting sources such as solar, wind, thermal, radiofrequency, human anatomy and mechanical vibration energy [1], [2], [3]. Researchers are exploring different types of systems which are circuit design, configuration and harvesting materials to optimize the amplitude of energy harvested so that it can be placed in multipurpose applications such as a human body, road, rail, pedestrian walkway, vibration machinery and others [4], [5].

This study focuses on harvesting energy from vibration energy using a piezoelectric transducer. The piezoelectric transducer will gain the vibration energy sources as an impact and change into alternating current (AC) source [6], [7], [8]. However, the extracted energy from vibration energy is not adequate to be directly applied to loads. Therefore, the AC-DC converter circuits design was investigated to extract the maximum power from the harvester and transfer it to the load circuit efficiently. Previous research has shown that S. wang et al. [9] used a full wave rectifier circuit that producing 11mW of output power at 590 Hz across an 18 k $\Omega$  resistor. Meanwhile, Goudarzi et al. [10] used a parallel SSHI to generate 6.049 mW at 20 Hz and H. C. Lin et al. [11] generated 7.8 mW at 45 Hz by using a parallel SSHI. Another research of power harvesting by L. H. Fang et al. [12] using parallel voltage multiplier was generated output voltages at 9.593V. Several reviews related to the AC-DC converter circuit can be found in literature [13], [14], [15].

The above studies are focused on the AC-DC converter circuit that generated power from piezoelectric. In this research, the AC-DC converter circuit was analyzed to find the effects affecting the combination with a different set of array configuration of the piezoelectric circuit. There are three equivalent circuits of piezoelectric was used in simulation to create several types of array piezoelectric connection which are 3 series (3S), 3 parallel (3P), 2 series 1 parallel (2S1P) and 2 parallel 1 series (2P1S). There are three different types of AC-DC converter circuit involved in this research. This circuit was chosen based on their performance from previous research related to the energy harvesting circuit. The three circuits considered were FWBR, PVM and P-SSHI.

## 2. The piezoelectric energy harvesting system

The block diagram which is an equivalent circuit of the piezoelectric energy harvesting system is shown in Fig. 1. It consists of five main parts which are the piezoelectric generator, AC-DC converter, DC-DC converter, energy storage device and a load [16], [17], [18]. The system can be constructed using a different method in order to increase system performance.

The different blocks have specific functions and are operational to produce useful electricity. The first block is the piezoelectric generator and also known as a piezoelectric sensor. The piezoelectric sensor is functional to convert the vibration energy into electrical energy. It is converted into electrical energy when stress is applied to the surface. The second block is the AC-DC converter circuit. The function of this block is to convert the AC source to the DC source using several types of AC-DC converter circuits. The third block is a DC-DC converter circuit that typically employs a DC-DC converter, mainly to match the source voltage with the battery charging level. The fourth block is storage that usually houses a battery to store the charge from the source. Therefore, the charge stored in the battery could be used for energizing the application.

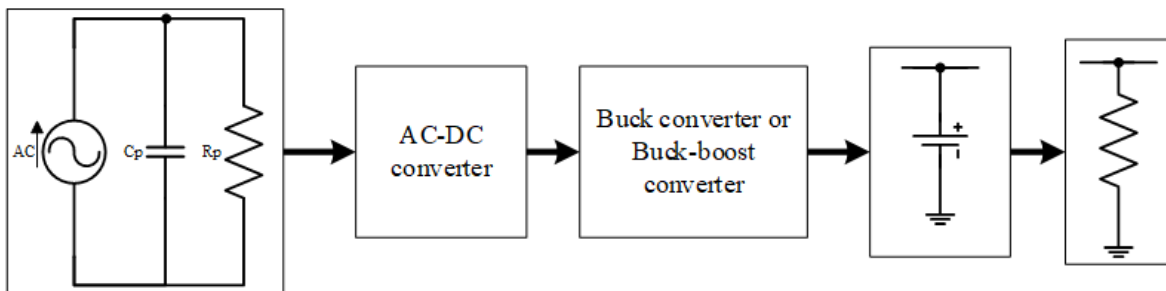
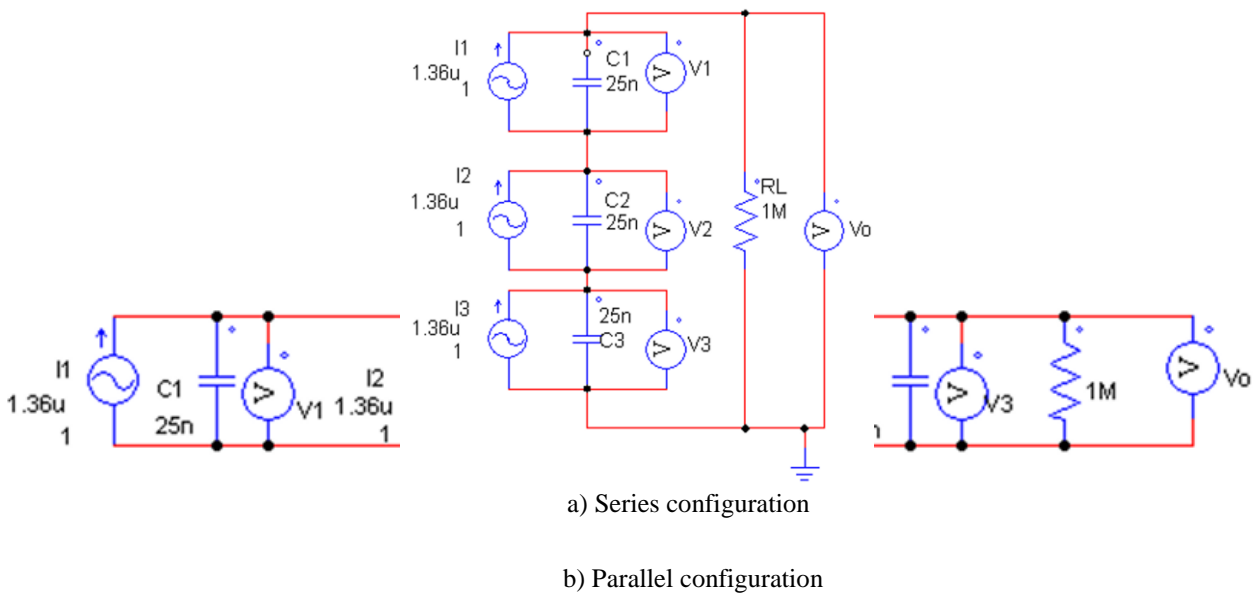
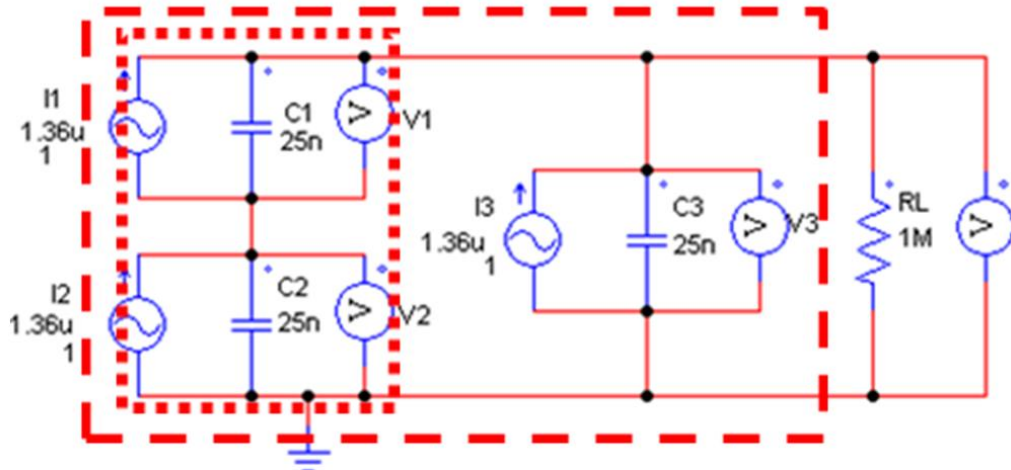


Fig. 1 - The basic block diagram of a piezoelectric energy harvesting system

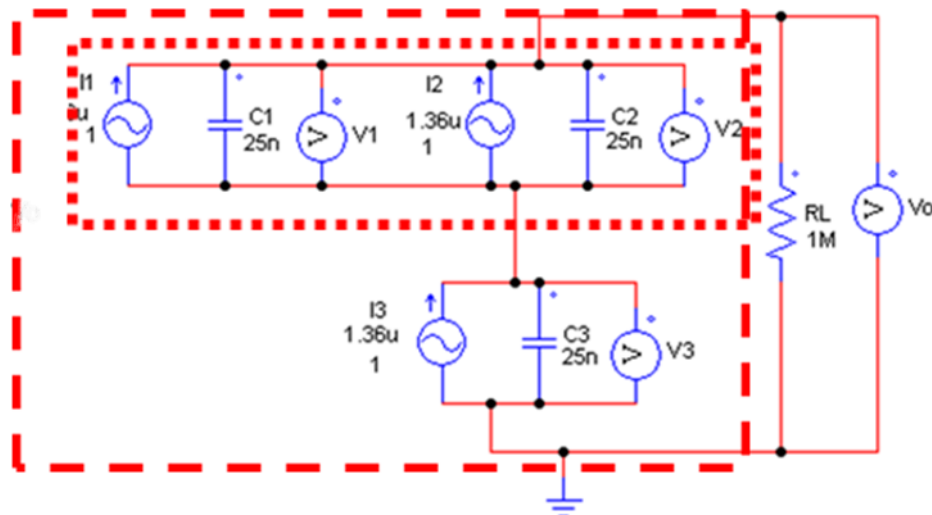
## 3. Types of array piezoelectric sensor and ac-dc converter circuits

The simulation by simulating an array of piezoelectric sensor connection which consisted of series (S), parallel (P), combination series-parallel (SP) and combination parallel-series (PS) combine with AC-DC converter circuit which are full wave bridge rectifier (FWBR), parallel SSHI (P-SSHI) and parallel voltage multiplier (PVM).





c) 2 Series 1 Parallel



d) 2 Parallel 1 Series

**Fig. 2 - Configuration circuit of piezoelectric sensor connection**

Fig. 2a shows the three equivalent circuits linked together in a series connection. This circuit also is known as the three series of piezoelectric connections. The three equivalent circuits were linked together in parallel connection as shown in Fig. 2b. This circuit also is known as the three parallel of piezoelectric connection.

Fig. 2c shows the equivalent circuits of array connection of two series one parallel circuit. This combination only used three piezoelectrics that were connected in two series (dotted square) and combined with one parallel (dash square). Fig. 2d shows the equivalent circuits of array connection of two parallel one series circuit. This combination only used three piezoelectrics that were connected in two parallels (dotted square) and combined with one series (dash square).

The Full Wave Bridge Rectifier (FWBR) is the basic circuit of the AC-DC converter. Fig. 3 shows the FWBR, the full wave diode bridge rectifier directly connected to the piezoelectric element that paralleled with a smoothing capacitor ( $C_s$ ) and load resistance ( $R_L$ ). The load current was only in the positive cycle because the  $D_1$  and  $D_2$  cannot be conducted simultaneously; similar to  $D_3$  and  $D_4$ . The positive voltage source flowed through the load when  $D_1$  and  $D_4$  were conducted and then, the negative voltage source flowed through the load when  $D_2$  and  $D_3$  were conducted.

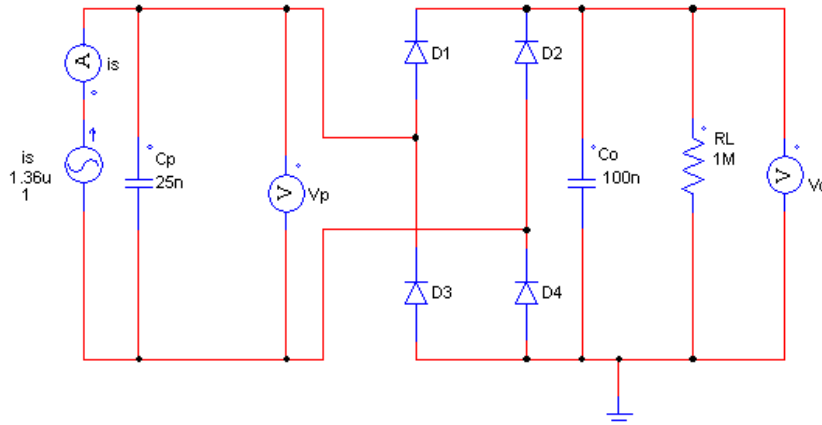


**Fig. 3 - The Full Wave Bridge Rectifier (FWBR) simulation circuit**

The second type was the Parallel Synchronized Switch Harvesting on Inductor (P-SSHI) circuit as shown in Fig. 4 where the P-SSHI and the piezoelectric had a large internal capacitance that required the impedance matching circuit to maximize the produced output power. The inductance value is selected to compensate the piezoelectric sensor clamped capacitor; however, the value cannot be automatically adjusted to the exciting frequency environment. Therefore, to resolve this problem, the method using the switching type charging circuit called SSHI was proposed. In SSHI, switches are implemented and it will operate synchronously with the vibration environment frequency to optimize the output power. When the vibration hits the piezoelectric sensor, the switch is operated in a very short time. It is found that during a short time the frequency of  $C_p$  will match the resonance frequency with an inductor ( $L_1$ ).

An inductor ( $L_1$ ) has been connected in series with switch  $S_1$  as in Fig. 4. The inductor functioned to passively flip the voltage flow across a capacitor. Therefore, in P-SSHI, the inductor was implemented to flip the voltage across  $C_p$ , eliminating the usage of the switch. The voltage and current waveforms related to the circuit are summarised as in Fig. 4.

During every half-cycle, as  $i_s$  changed direction, the switch  $S_1$  was active (ON), allowing the inductor to flip the voltage across  $C_p$ . The switch was turned OFF when the current in the inductor reduced to zero. When the current flowed through  $L_1$ , the  $C_p$  was in an ideal state, thus the voltage flipped perfectly. However, voltage inversion magnitude was bounded by the resistance through the  $L_1$  path. In order for the current to flow to the output, the piezoelectric current needed to charge up  $C_p$  using the flipped voltage to around  $2V_D$ . This was done to reduce the loss of charges and allow accumulated charges to flow into the output capacitor without charging or discharging  $C_p$ .

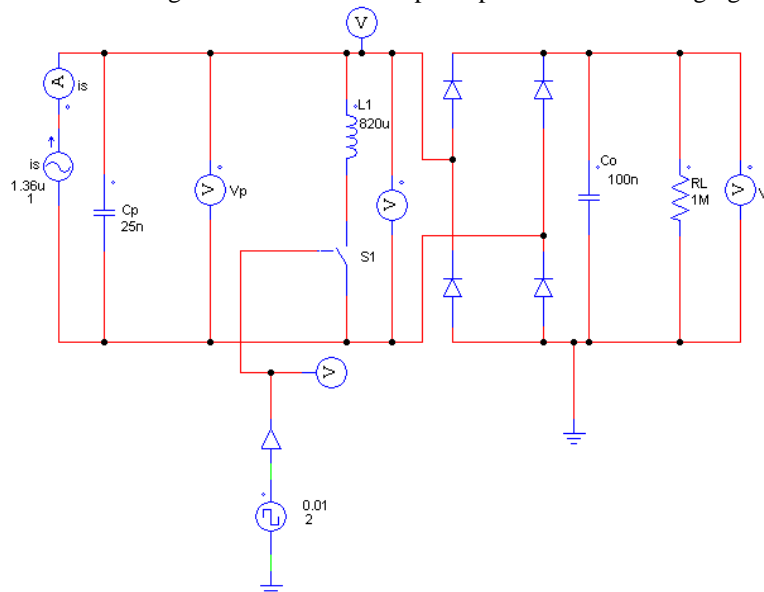


**Fig. 4 - Parallel SSHI (P-SSHI) simulation circuit**

The third AC-DC circuit was the Parallel voltage multiplier (PVM) circuit as shown in Fig. 5 which included stage voltage storage capacitors ( $C_3$ ), diodes and pumping capacitors ( $C_1$  and  $C_2$ ). The pumping capacitors were pre-charged in parallel when the input sinusoidal signaled at negative half cycle and then delivered current to the storage capacitors and tank  $C_o$  that was connected to the ground node at the next positive half cycle. The signal in the half wave voltage multiplier was only at a half period when the input current from the piezoelectric sensor that entered the diodes.

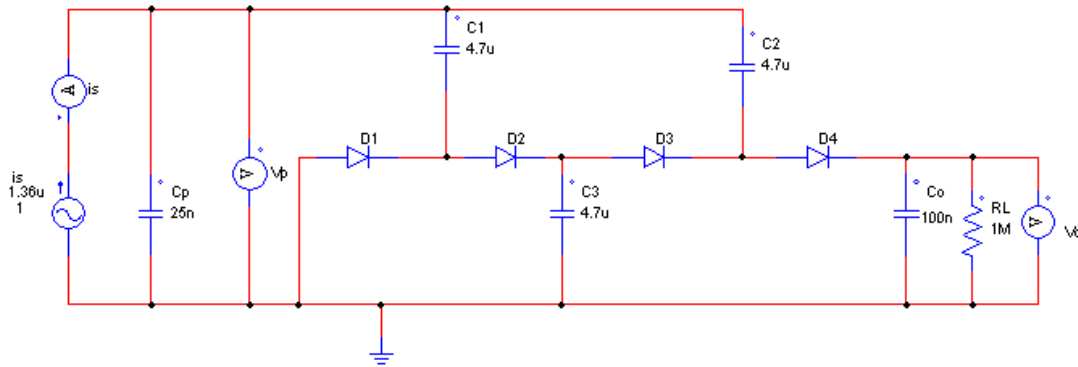


Fig. 5 - Parallel voltage multiplier (PVM) simulation circuit

#### 4. Results and discussion

##### 4.1 The simulation result of various piezoelectric sensor connection with an AC-DC converter circuit

The simulation is done with the combination of piezoelectric array sensor connection with an AC-DC converter circuit applied with a load resistances of 1 MΩ and 10 kΩ. These two resistor value were the selected as a higher resistance will allow less charge to flow, which make the circuit with higher resistance has less current and higher voltage flowing through it. The low resistance will allow a high charge to flow, therefore the circuit will produce a higher current and low voltage. There were three types of circuits used namely PVM, P-SSHI and FWBR connected with 1 piezoelectric, 3S, 3P, 2P1S and 2S1P.

Fig. 6 and 7 show the simulated result using various piezoelectric sensor connections with an AC-DC circuit namely PVM, P-SSHI and FWBR. As can be seen from Fig. 8, the highest power output was observed at 3 parallel connection of piezoelectric using P-SSHI at 7.87μW across 1 MΩ. It can be seen that the power output generated from P-SSHI using 3 piezoelectric sensors in parallel connection was 85.9% higher than PVM and 15.88% higher than FWBR.

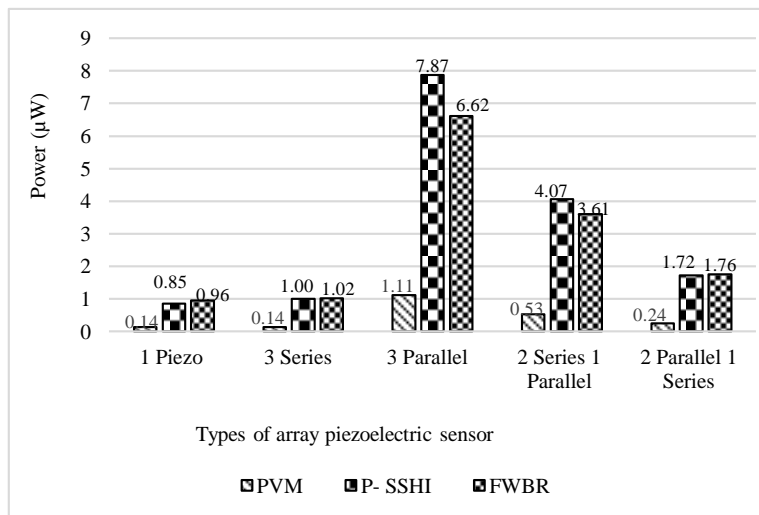


Fig. 6 - Output power generation between AC-DC circuit and different types of array piezoelectric connection across 1 MΩ simulation

Meanwhile, by using the load resistance of 10kΩ, the output power generated from the 3 parallel connection of piezoelectric by using FWBR was 165.78 pW. In view of the results obtained, the output power values were shown to be slightly different for all types of combination circuits. In this analysis, the output power values using 3 parallel connection of piezoelectric produced by FWBR circuit was 83.83% higher than PVM and 16.14% higher than P-SSHI.

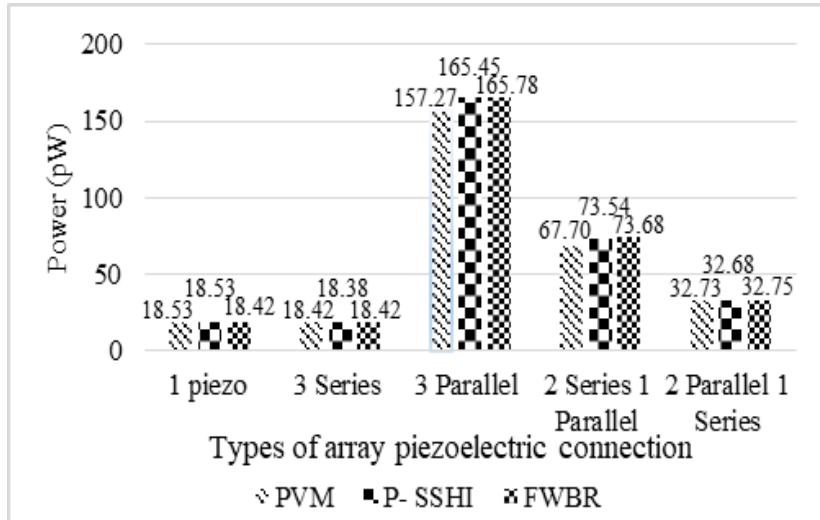


Fig. 7 - Output power generation between AC-DC circuit and different type of array piezoelectric connection across the 10kΩ simulation

#### 4.2 The simulation result of P-SSHI

Fig. 8 shows the waveform of piezoelectric voltage ( $V_p$ ) by using P-SSHI with 3 parallel arrays of piezoelectric across the 1 MΩ load resistor. The power delivered to the load maximized with the reduction of time duration in charging the  $C_p$  value. The waveform is shown when using P-SSHI combined with 3 parallel array connections across 1 MΩ where the charging time of  $C_p$  was short compared to using the one piezoelectric as shown in Fig. 8.

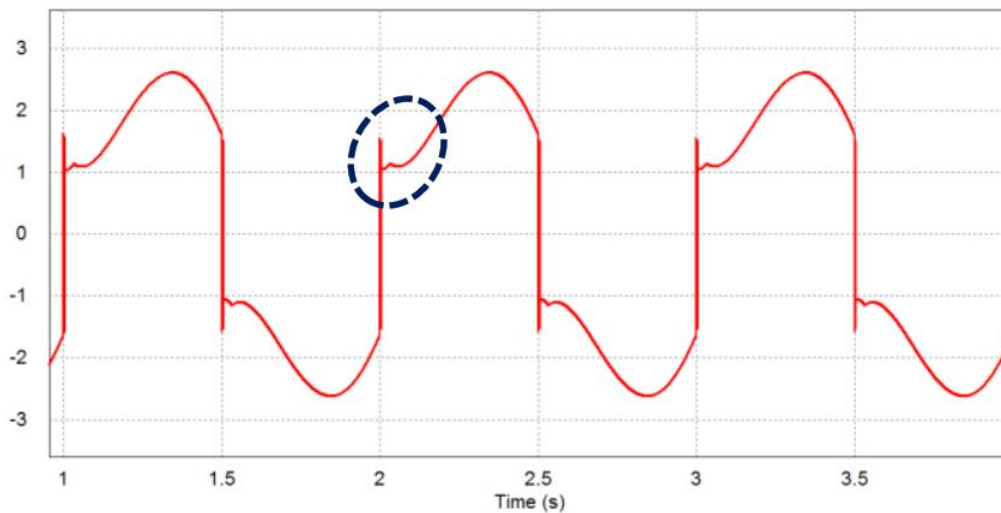
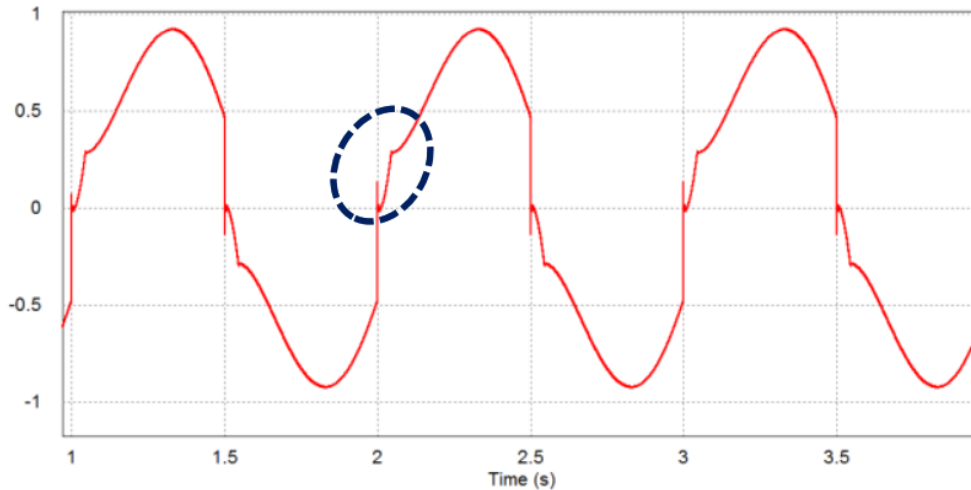


Fig. 8 - The voltage waveform P-SSHI and 3 piezoelectric sensors in parallel arrays across 1 MΩ load resistance

Fig. 9 shows the waveform of  $V_p$  using P-SSHI with one piezoelectric sensor connection across 1 MΩ of the load resistor. The waveform shows that by using one piezoelectric with 1 MΩ of load resistor, the charging time of  $C_p$  increased and affected the shape of the waveform. In addition, with the affected  $V_p$  waveform, the output extracted from piezoelectric also decreased.



**Fig. 9 - The waveform of piezoelectric voltage using P-SSHI with one piezoelectric across 1 M $\Omega$  load resistance**

## 5. Conclusion

The investigation with simulating the AC-DC converter circuit by connecting the 3P array of piezoelectric with three different types of AC-DC converter. The chosen converters were PVM, FWBR and P-SSHI. The simulation result showed that the maximum power output was produced by 3P connected with P-SSHI using 1 M $\Omega$  load resistor at 4.52 $\mu$ W. As can be seen, the power output generated from P-SSHI at 3P connection was 46.33% higher with PVM and 35.31% higher with FWBR. However, when the load resistor was 10 k $\Omega$ , the maximum output power was generated using the 3P array piezoelectric by connecting with the FWBR circuit. This was due to the effect of the charging time  $C_p$  increasing which affected the shape of the  $V_p$  waveform. Furthermore, due to the affected  $V_p$  waveform, the output extracted from piezoelectric was decreased.

## Acknowledgement

The authors would like to thank Universiti Malaysia Perlis (UniMAP) and Ministry of Education Malaysia for providing research facilities and funding for the project via Fundamental Research Grant Scheme (Grant No. 9003-00695 and FRGS/1/2018/TK04/UniMAP/02/5).

## References

- [1] Ilyas, M. A., & Swingler, J. (2015). Piezoelectric energy harvesting from raindrop impacts. *Energy*, 90, 796–806
- [2] Lien, I. C., Shu, Y. C., Wu, W. J., Shiu, S. M., & Lin, H. C. (2010). Revisit of series-SSHI with comparisons to other interfacing circuits in piezoelectric energy harvesting. *Smart Materials and Structures*, 19(12), 125009
- [3] Ali, S., Zaidi, R., Afzal, A., Hafeez, M., Ghogho, M., & McLernon, D. C. (2015). Solar Energy Empowered 5G Cognitive Metro-Cellular Networks. *IEEE Communications Magazine*, 53(7), 70–77
- [4] Jabbar, H., Hong, S. Do, Hong, S. K., Yang, C. H., Jeong, S. Y., & Sung, T. H. (2018). Sustainable micro-power circuit for piezoelectric energy harvesting tile. *Integrated Ferroelectrics*, 183(1), 193–209
- [5] Song, Y., Yang, C. H., Hong, S. K., Hwang, S. J., Kim, J. H., Choi, J. Y., Ryu, S. K., & Sung, T. H. (2016). Road energy harvester designed as a macro-power source using the piezoelectric effect. *International Journal of Hydrogen Energy*, 41(29), 12563–12568
- [6] Calìò, R., Rongala, U., Camboni, D., Milazzo, M., Stefanini, C., de Petris, G., & Oddo, C. (2014). Piezoelectric Energy Harvesting Solutions. *Sensors*, 14(3), 4755–4790
- [7] Tian, W., Ling, Z., Yu, W., & Shi, J. (2018). A Review of MEMS Scale Piezoelectric Energy Harvester. *Applied Sciences*, 8(4), 645–665
- [8] Wang, Z., Pan, X., He, Y., Hu, Y., Gu, H., & Wang, Y. (2015). Piezoelectric Nanowires in Energy Harvesting Applications. *Advances in Materials Science and Engineering*, 2015, 1–21
- [9] Wang, S., Lam, K. H., Sun, C. L., Kwok, K. W., Chan, H. L. W., Guo, M. Sen, & Zhao, X. Z. (2007). Energy harvesting with piezoelectric drum transducer. *Applied Physics Letters*, 90(11), 2007–2009
- [10] Goudarzi, M., Niazi, K., & Besharati, M. K. (2013). Hybrid Energy Harvesting From Vibration and Temperature Gradient By Pzt and Pmn-0 . 25Pt Ceramics. 16(January 2013), 55–65
- [11] Lin, H. C., Wu, P. H., Lien, I. C., & Shu, Y. C. (2013). Analysis of an array of piezoelectric energy harvesters connected in series. *Smart Materials and Structures*, 22(9), 94026
- [12] Hui, L., Idris, S., Hassan, S., Abd, R., & Isa, M. (2017). Exploring Piezoelectric for Sound Wave as Energy Harvester. *Energy Procedia*, 105, 459–466

- [13] Mustapha, A. A., Ali, N. M., & Leong, K. S. (2013). Experimental comparison of piezoelectric rectifying circuits for energy harvesting. Proceeding - 2013 IEEE Student Conference on Research and Development, SCOReD 2013, 556–559
- [14] Chen, X. R., Yang, T. Q., Wang, W., & Yao, X. (2012). Vibration energy harvesting with a clamped piezoelectric circular diaphragm. *Ceramics International*, 38(SUPPL. 1), S271–S274
- [15] Wang, W., Huang, R. J., Huang, C. J., & Li, L. F. (2014). Energy harvester array using piezoelectric circular diaphragm for rail vibration. *Acta Mechanica Sinica*, 30(6), 884–888
- [16] Do, X. D., Han, S. K., & Lee, S. G. (2014). Optimization of piezoelectric energy harvesting systems by using a MPPT method. 2014 IEEE 5th International Conference on Communications and Electronics, IEEE ICCE 2014, 309–312
- [17] Mohamad, T. N. T., Sampe, J., & Berhanuddin, D. D. (2017). Architecture of micro energy harvesting using hybrid input of RF, thermal and vibration for semi-active RFID tag. *Engineering Journal*, 21(2), 183–197
- [18] Sarker, M. R., Mohamed, A., & Mohamed, R. (2016). Vibration Based Piezoelectric Energy Harvesting Utilizing Bridgeless Rectifier Circuit. *Jurnal Kejuruteraan*, 28(1), 87–94